Self-Association of Naphthalene at the Air−Ice Interface†

D. Ardura,‡ T. F. Kahan,‡ and D. J. Donaldson*,‡,§

Department of Chemistry, University of Toronto, 80 Saint George Street, Toronto, Ontario, Canada M5S 3H6, and Department of Physical and Environmental Sciences, University of Toronto, Scarborough, Ontario, Canada

Received: December 24, 2008; Revised Manuscript Received: April 7, 2009

We present a molecular dynamics study of the interactions between two molecules of naphthalene present at air−water versus air−ice interfaces. In agreement with the inference from our previous experimental work [Kahan, T. F.; Donaldson, D. J. *J. Phys. Chem. A* **2007**, *111*, 1277], the results suggest that self-association of the molecules is more likely to take place on the ice surface than on the water surface. A shorter average distance between the two naphthalene molecules, in conjunction with a stronger interaction energy and free energy of association, point to a stronger tendency to self-associate on ice than on water. The distinct behavior at the two interfaces appears be due to more favorable interactions between naphthalene molecules on liquid water surfaces than on ice surfaces.

Introduction

Organic pollutants such as polycyclic aromatic hydrocarbons (PAHs) are found in snow from both urban[1−9] and remote[2,4,7,10−21] regions. In addition to being important physical sinks, snowpacks can act as reaction substrates for these compounds. Several laboratory studies have shown that organic pollutants undergo photochemical and heterogeneous reactions in snow and ice.[22−32]

Physical and chemical processes occurring at the air−ice interface are often assumed to be well described by those occurring at a cold air−water interface. This is because at temperatures relevant to Earth's atmosphere, the structure of the ice matrix breaks down near the interface, and water molecules adopt more random orientations. This disordered region is commonly referred to as a quasi-liquid layer (QLL). However, this approach stems from the lack of understanding of the physical properties of the QLL and from the lack of *in situ* studies of processes occurring there. Of the few studies that have compared reaction kinetics of organic pollutants in ice and in water, the majority[23,25,26] suggest that this assumption is not accurate: Reactivities can differ by over an order of magnitude in the two media.

Using glancing-angle laser-induced fluorescence (LIF), we have measured electronic spectra of PAHs adsorbed at air−ice and air−water interfaces.[25,26,33] Figure 1 shows emission spectra of anthracene at the air−water interface and of naphthalene in bulk water as well as emission spectra of both PAHs at the air−ice interface. Red shifts in the emission spectra of the PAHs on ice compared to those observed on or in aqueous solution are evident. These red-shifted spectra closely resemble excimer emission spectra of the two species and are thus indicative of self-association.[34−36] Figure 1a shows that only after close to 2 h of gas phase deposition does anthracene's emission spectrum at an air−water interface shift to that of the self-associated species. By contrast, on ice this is the only emission we see, even at very short deposition times. We have also observed phenanthrene emission indicative of self-association on ice,[26]

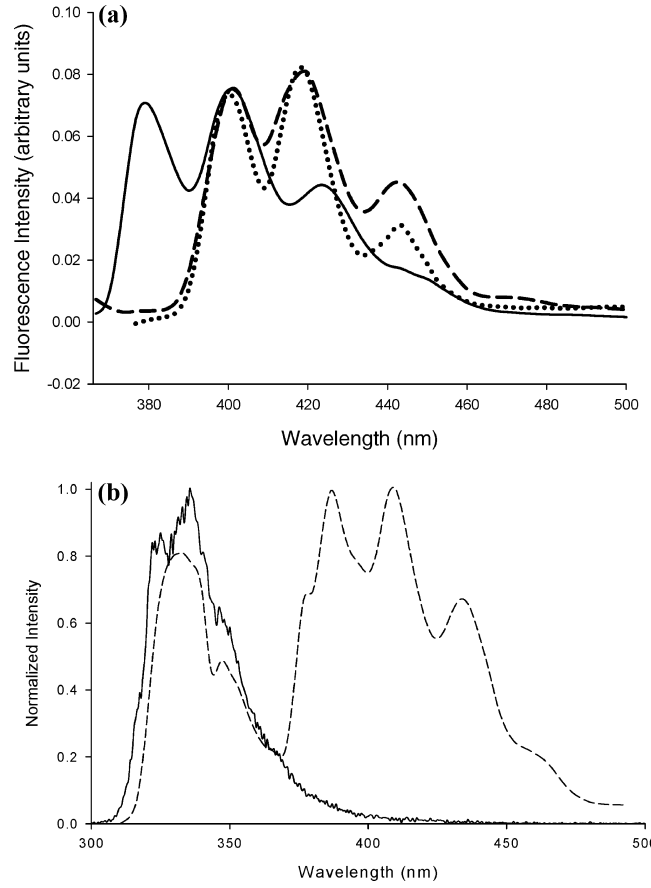

Figure 1. Fluorescence spectra of (a) anthracene deposited on a water surface for 30 min (solid trace), 115 min (dashed trace), and on a −15 °C ice surface for 10 min (dotted trace); and (b) naphthalene in aqueous solution (solid trace) and at the air−ice interface of a frozen solution at −15 °C (dashed trace). These images are reproduced from ref 25. Copyright 2007 American Chemical Society.

while on the liquid water surface, only monomeric emission is observed. The enhanced self-association of PAHs on ice does not appear to be an effect of temperature: we observe the same evidence for self-association at −2 and −30 °C. These observations suggest that, at least in the case of adsorbed PAHs, the

† Part of the "Robert Benny Gerber Festschrift".

* To whom correspondence should be addressed. E-mail: jdonalds@chem.utoronto.ca.

‡ Department of Chemistry.

§ Department of Physical and Environmental Sciences.

10.1021/jp811385m CCC: $40.75
Published on Web 04/23/2009

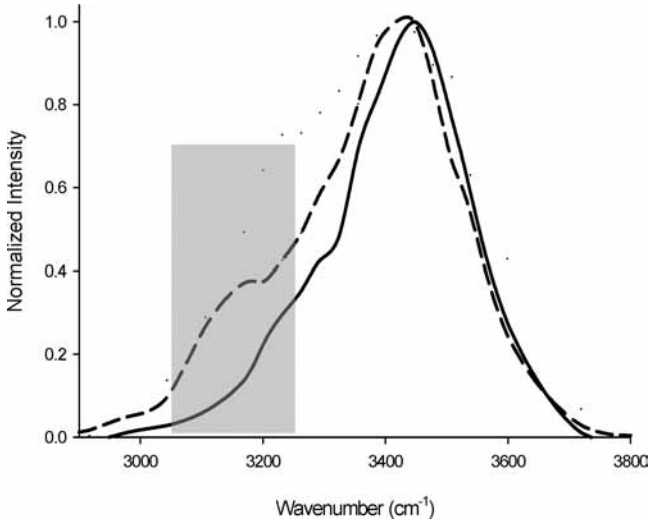

Figure 2. Glancing-angle Raman scattering of the OH-stretch of water at a room temperature air−water interface (solid trace) and an air−ice interface at −15 °C (dashed trace). The highlighted area indicates the spectral region associated with strongly hydrogen-bonded water.[39,67] This image is reprinted with permission from ref 33. Copyright 2009 American Chemical Society.

QLL does not present a solvation environment similar to that present at the surface of liquid water.

In order to explain these observations, we suggested[26] that the enhanced self-association observed on ice compared to that on liquid water could be due to a less favorable hydrogen-bonding environment at the air−ice interface. Figure 2 shows glancing-angle Raman spectra acquired at air−ice and air−water interfaces.[33] The enhanced intensity at 3200 cm^{-1} on ice suggests that there is enhanced water−water hydrogen-bonding at that surface and therefore fewer available free OH-groups, compared to those at a liquid water surface. A sum-frequency generation (SFG) study[37] also indicated different hydrogen-bonding environments at air−ice and air−supercooled water interfaces; in those experiments, the surfacial OH-bonds of ice showed a lesser degree of orientational order than did those of water. Although the structure of the water molecules at air−aqueous interfaces has been studied extensively experimentally (readers are referred to refs 38−41 for reviews of these studies), and the structure of air−ice interfaces has also been investigated in recent years,[42,43] we are not aware of any studies other than those discussed above that directly compare the hydrogen-bonding nature of the two environments.

In recent years, molecular dynamics simulations that include the presence of a QLL have been developed.[44−49] A few studies have examined the adsorption of single molecules of acetone,[50] methanol and formaldehyde,[51] acetic acid,[52] and phenanthrene[53] to ice surfaces. These studies agree fairly well with available experimental studies, for example they predict accurate enthalpies of adsorption. However, our experimental observations suggest that solute−solute interactions could be different at air−ice interfaces compared to those at air−water interfaces. This implies that more than one adsorbate molecule may need to be included in order to properly describe the fate of trace gases adsorbed to ice. In the present study, we investigated the binding and self-association of naphthalene at ice and liquid water surfaces using molecular dynamics simulations of two naphthalene molecules, with the aim of understanding whether differences in the hydrogen-bonding nature of liquid and solid water surfaces can explain the observed self-association of PAHs on ice.

Computational Details

The air−water interface was modeled by a 24.6(x) × 24.4(y) × 200.0(z) Å parallelepiped solvent box water slab consisting of 1575 water molecules. An I_h ice slab of 24.0(x) × 23.8(y) × 200.0(z) Å was used for the MD simulations of the air−ice interface; it contained 1476 water molecules. On the basis of the results from a recent study of the thickness of the QLL,[54] the simulation box for the ice interface was built with five bilayers of free water molecules corresponding to a QLL thickness of about 10 Å, placed on two bilayers of ice. Both the air−water and air−ice systems were equilibrated for 4 ns in an NVT ensemble, after which a 4 ns production run was carried out at an average temperature of 270 K, which was maintained using the Berendsen scheme[55] with a coupling constant of 0.5 ps. We used the same simulation temperature for both model surfaces in order to avoid any effects due merely to different temperatures of the two substrates. Periodic boundary conditions were applied in all three dimensions. The z-axis was perpendicular to the water surface and the one or two naphthalene solute molecules were placed above the slab. All bond lengths were constrained to their equilibrium values using SHAKE.[56] A smooth particle mesh Ewald method with an interaction cutoff of 10 Å was used to account for the long-range Coulomb interactions.[57] Liquid water molecules were described using the SPC/E model, which has been successfully applied in the study of the adsorption of PAHs at the air−water interface.[58,59] TIP5P was used to model the water molecules of the ice slab (both for the fixed water molecules of the two bilayers of ice and the free molecules above which form the QLL). This approach has been used previously by Domine et al.[53] to simulate the adsorption of phenanthrene to an ice surface;

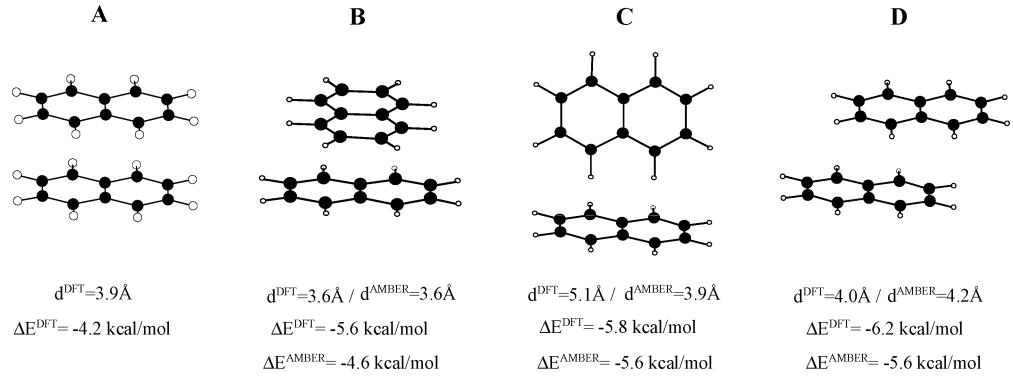

Figure 3. Different possible configurations of the naphthalene dimer in the gas phase. The distance between the center of mass of each structure and the interaction energy at both DFT and MM (Amber) levels of theory are given.

it gives the correct melting point for ice.[14] The bond lengths, bond angles, and dihedral parameters were obtained from the AMBER force field.[60] The atomic charges of the naphthalene atoms were evaluated from an optimized structure with the RESP method after an *ab initio* HF/6-31G* calculation by fitting the electrostatic potential at points selected according to the Merz−Singh−Kollman scheme.[61] All MD simulations were performed using the AMBER 10.0 program package.[62]

A DFT study[63] using long-range corrections (LC-DFT) with the van der Waals−Andersson−Langreth−Lundqvist functional found four different relevant minima for the naphthalene−naphthalene complexes; these are shown in Figure 3. The distances between the centers of mass (CM) in each case range from 3.6 Å in complex B to 5.1 Å in complex C, and the interaction energies range from −4.2 kcal/mol (complex A) to −6.2 kcal/mol (complex D). In order to benchmark the AMBER force field against these π-aromatic interactions, we compared the geometry and energy of DFT results to those we found at the molecular mechanics level using the AMBER force field. We found three minima comparable to the structures B, C, and D from the QM study. The distances between the CM of the naphthalenes were 4.1, 3.9, and 4.2 Å, respectively, and the interaction energies were −4.6 kcal/mol for complex B; complexes C and D were isoenergetic with an interaction energy of −5.6 kcal/mol. With this level of agreement with the LC-DFT calculations, we believe that AMBER is a suitable force field for the present investigation.

The umbrella sampling procedure was used to obtain the potential of mean force (PMF) for naphthalene−naphthalene interactions through a biased potential of the form

$$U = k_0(r - r_0)^2$$

where k_0 was 5 kcal mol^{-1} Å^{-2}. This potential constrained the distance between the center of mass of the two naphthalene molecules to a small range of values surrounding the central value r_0 (the sampling window). The sampling was carried out in 33 windows, which covered a range from 3.0 to 11.0 Å with a gap distance of 0.25 Å. In every window, a 500 ps sampling was performed. The umbrella sampling histograms were unbiased and combined using the weighted histogram analysis method (WHAM)[64,65] to generate the PMF on each surface.

Results and Discussion

The adsorption of PAHs to the air−water interface has been studied recently by Jungwirth et al.[58,59] by means of MD simulations. For all of the compounds studied there, surface free energy minima were found corresponding to the adsorption of the gas-phase species to the water surface. The interaction of the PAHs with the surface depends on the size of the compound: the higher the molecular weight, the stronger the interaction with the surface. For example, the adsorption free energy reported in ref 58 for benzene is 3.7 kcal/mol; this increases to 6 kcal/mol for naphthalene and 7.8 kcal/mol for the three-ringed PAH phenanthrene. These simulations all predict that the PAHs tend to lie parallel to the water surface. A recent study[53] of the adsorption of phenanthrene on ice did not report adsorption free energies but showed similar results in terms of the orientation of the PAH with respect to the surface. The binding energies given in ref 53 do indicate a stronger interaction with the liquid water surface than with the ice surface.

We ran MD simulations of a single naphthalene molecule on ice and liquid water substrates and evaluated the interaction energy between the adsorbate and the surface. We took a snapshot from the production run every 10 ps and performed a single point calculation on a cluster formed by the naphthalene and all of the water molecules within a radius of 10 Å around it. The average interaction energies with the ice and the water surfaces are 9.7(0.2) kcal/mol and 10.8(0.2) kcal/mol, respectively. The numbers within parentheses (here and in the following) are the standard errors, given by [standard deviation/(number of snapshots)$^{1/2}$]. The naphthalene tends to remain flat on the surface, in agreement with the other studies mentioned above.[53,58,59] Consistent with the MD result for phenanthrene on water and ice surfaces,[53] the binding energy is somewhat higher on the water surface than on the ice surface.

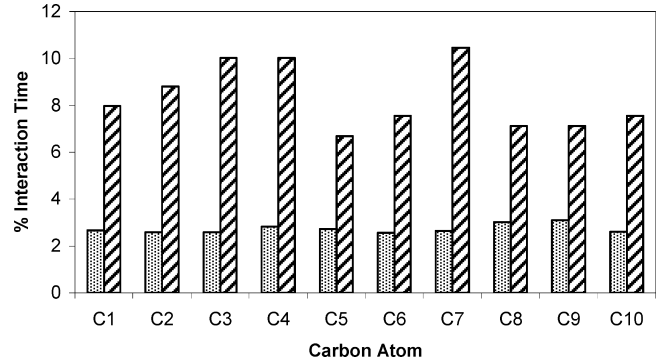

Figure 4. Percentage of the production time in which each naphthalene carbon atom interacts with a surfacial water hydrogen atom at the air−ice interface (dotted area) and at the air−water interface (diagonal striped area). Interactions are defined as intermolecular distances between the C and H atoms of less than 6 Å.

A difference in the nature of the interaction of naphthalene with ice and water surfaces is seen in the specific interactions between the surfacial water hydrogens and the carbon atoms in the naphthalene. Figure 4 shows the percentage of time of the production run in which the different carbon atoms of the naphthalene are interacting with one of the hydrogens of the surfacial water molecules. On average, each carbon atom interacts for 8.3% of the production run with a surface hydrogen on liquid water, but only for 3.0% with a surface hydrogen on ice. In a typical interaction with the surface, the average distances between one water hydrogen on the surface and the center of one of the naphthalene rings are 2.8(0.2) and 4.8(0.3) Å on water and on ice, respectively. This finding implies different degrees of hydrogen bonding at the two substrates and is consistent with our hypothesis that the enhanced self-association of PAHs at ice surfaces compared to water surfaces could be due to differences in the hydrogen-bonding natures of the two substrates.

According to our experimental observations, PAHs exhibit self-association on ice surfaces, whereas this is only observed after significant loading of these adsorbates onto water surfaces. We followed the distance between the center of mass of two naphthalenes on a water surface and on an ice surface at a simulation temperature of 270 K for a total of 4 ns. As displayed in Figures 5a (water) and 6a (ice), in both cases the naphthalene−naphthalene distance ranges between a minimum value of 4 Å and a maximum of 16 Å. However, there is a marked difference in the average values extracted from the trajectories of the systems: 9.3(0.2) Å on the water surface and 7.5(0.1) Å on the ice surface. The significantly smaller average separation indicates stronger average interactions between the two naphthalenes on ice than on water. The fluctuations in the distance between the two naphthalenes are also larger at the water surface than at the ice surface, as evidenced by the

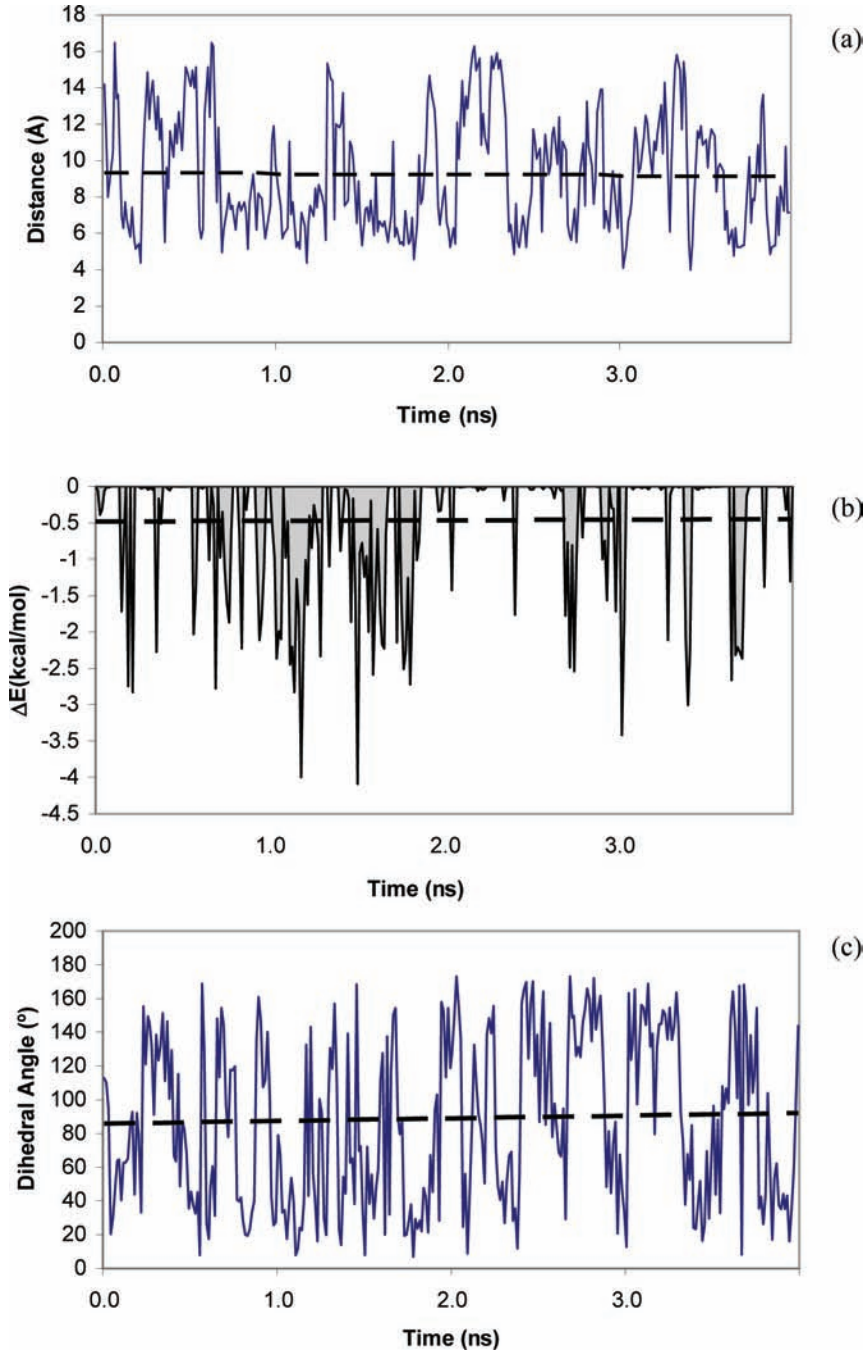

Figure 5. (a) Distances between the centers of mass of the two naphthalenes; (b) stabilization energy of the naphthalene complex; and (c) dihedral angle between the two naphthalenes at the air−water interface. The average value is indicated by a dashed line.

larger standard deviation about the average interadsorbate distance found for the water interface (3.2 Å) than the ice surface (2.2 Å).

To further explore the nature of any complex formed on the surface, we also followed trajectories on both surfaces in terms of the naphthalene−naphthalene interaction energy. For this purpose, we extracted the relative positions of the two naphthalenes every 10 ps and performed a single point calculation at the same level of theory as the MD in order to calculate the energy of the self-associated species; this was compared to two times the energy of one naphthalene molecule. Consistent with the average distances obtained on the two substrates, stronger interactions are observed on the ice surface. Figures 5b and 6b illustrate the interaction energies on the water and ice surfaces, respectively, calculated along the production runs. The average values, over the 4.0 ns trajectories, are 1.36(0.08) kcal/mol on ice and 0.48(0.05) kcal/mol on the water surface. The strongest interaction, approximately 3 kcal/mol, is obtained on ice during the time of closest approach, between 1.2 and 2.5 ns of the trajectory shown in Figure 6.

To compare the free energy profiles at the air−water and air−ice interfaces, we computed the PMF by choosing the distance between the center of mass of each naphthalene as the reaction coordinate. As displayed in Figure 7, the PMF curve corresponding to the association of the two naphthalene molecules on the ice surface presents a minimum located at an intermolecular distance of approximately 5 Å. From this point, the energy increases monotonically with distance until the complex fully dissociates. The free energy of formation of the complex on ice is −2.00 kcal/mol. In the case of the water

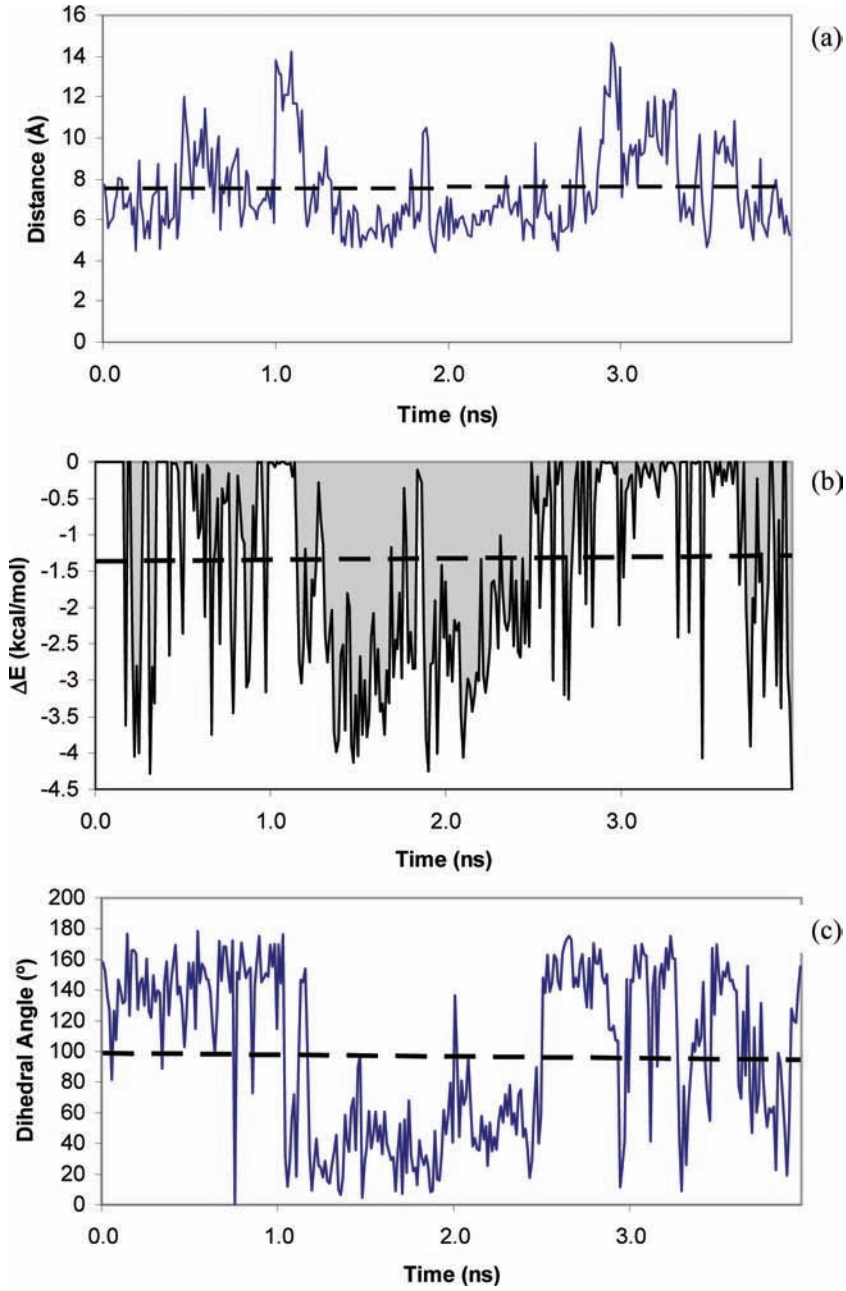

Figure 6. (a) Distances between the centers of mass of the two naphthalenes; (b) stabilization energy of the naphthalene complex; and (c) dihedral angle between the two naphthalenes at the air−ice interface. The average value is indicated by a dashed line.

surface, the dissociation curve displays a flat area between 5 and 6 Å when the complex is formed. Unlike that for the ice surface, the curve presents a ~1 kcal/mol barrier to association of the two naphthalenes at a distance of ~8 Å. The presence of this free energy barrier may well act to inhibit complex formation on the water surface. The overall free energy of association is smaller on this surface than on ice: only −1.08 kcal/mol. By comparing the free energies of association of naphthalene−naphthalene complexes on the two surfaces, we can conclude that, in agreement with the binding energies on both surfaces, the complex is more likely to form on the ice surface than on the water surface.

As discussed above, previous high level *ab initio*[66] and DFT[63] calculations found four different configurations for the naphthalene dimer in the gas phase (see Figure 3). The most stable arrangement corresponds to the parallel displaced structure, (type D in Figure 3) with an interaction energy of 6.2 kcal/mol. To describe the geometry of the complex on the ice surface, we evaluated the dihedral angles between the two naphthalenes along trajectories on water and ice. Figures 5c and 6c display the results on the respective substrates. During the longest period of interaction on the ice surface (i.e., between 1.2 and 2.5 ns), the average dihedral angle is 43.5(0.6)°, and the average distance between the center of mass of each naphthalene is 6.2(0.1) Å. These geometric data reveal that both the parallel configuration through the $\pi-\pi$ stacking interactions and the T-shape arrangement by means of CH$-\pi$ interaction between the hydrogen of one of the naphthalenes and the π cloud of the other are important in describing the structure of the complex on the ice surface. In Figure 8, we show a snapshot of the complex, extracted during the longest period of interaction. In this snapshot, the distance between the center of mass of each naphthalene is 5.6 Å, the dihedral angle between them is 46.2°, and the interaction energy of the complex is 4.1 kcal/mol.

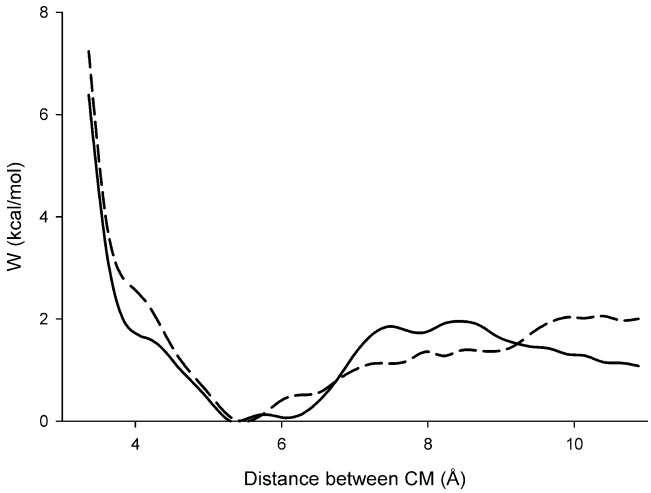

Figure 7. Potential of mean force as a function of the distance between the centers of mass of the naphthalene molecules at the air−water interface (—) and at the air−ice interface (---).

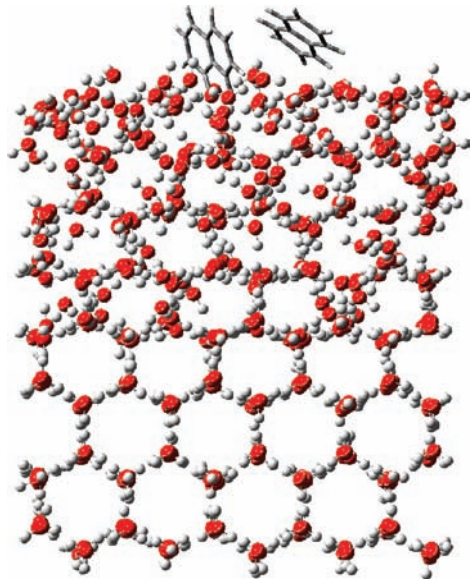

Figure 8. Snapshot of the naphthalene complex on the ice surface extracted from the MD simulation.

As displayed in Figure 5c, on water the naphthalene molecules do not exhibit a preferred relative orientation as they do on ice. Rather, the dihedral angle fluctuates randomly about the mean of close to 90°. Inspection of Figure 5 as a whole indicates that at the water surface, the two naphthalenes act independently of one another, in spite of stronger *individual* binding to the surface. By contrast, Figure 6 shows that on ice there is an important internaphthalene interaction possible when the two molecules are close enough, adapting a favorable relative configuration.

The closer approach and favorable geometry that may occur on ice also appears to strengthen the naphthalene pair's binding to the ice surface. The total average interaction energy of the complexed naphthalenes (extracted during the interval between 1.2 and 2.5 ns of the simulation) with the ice surface is 25.7(0.3) kcal/mol, compared to an energy of 19.4 kcal/mol for two isolated naphthalene molecules on the same surface. This enhancement in surface binding energy for the complex could mean that partitioning models based on properties of the monomer may not always be accurate on ice or on other substrates where self-association occurs.

Conclusions

An analysis of the energetics of clusters extracted from MD simulations with one molecule of naphthalene reveals that the energy of adsorption is somewhat stronger on liquid water than on ice, consistent with previous MD results for phenanthrene adsorption to these substrates.[53] Clear differences in the behavior of two naphthalene molecules on ice versus on water surfaces were observed in MD simulations: the formation of a complex between the two naphthalene molecules is more likely to occur on ice than on water, and the interadsorbate interactions are stronger on ice, consistent with experimental observations. Since both simulations were carried out at the same temperature (270 K), we confirm that the self-association of PAHs on ice is not a temperature effect. Rather, the results suggest that the distinct behavior of PAHs at air−water and air−ice interfaces is due to the different hydrogen-bonding natures of the two substrates.

These observations have implications for our understanding of the QLL's role as a reaction substrate and for the conclusions we extract from MD simulations. Self-associated PAHs often absorb at longer wavelengths than the monomeric species. We have previously suggested the importance of this in terms of the photolysis of naphthalene on ice:[25] its photolysis kinetics are enhanced by an order of magnitude on ice compared to in liquid water. The present results reinforce our suggestion that this may be due to an increased fraction of absorption in the actinic region by the strongly interacting species.

In terms of understanding the fate of molecules in the QLL compared to their fate in liquid water, our results suggest that including more than one molecule in theoretical studies may be necessary. We see qualitatively similar behavior for a single naphthalene molecule on the water and ice surfaces, but clear differences are observed when two molecules are present. The most important conclusion that we draw from this investigation is that the QLL is not always well represented by liquid water and that caution should be used when drawing comparisons between the two media in the absence of experimental evidence.

Acknowledgment. We are grateful to the MRQ group at the University of Oviedo for CPU time and to Professor Dimas Suárez for helpful suggestions. D.A. acknowledges a postdoctoral fellowship (POST07-25) from the Consejería de Educación y Ciencia of the Principado de Asturias (Plan de Ciencia, Tecnología e Innovación (PCTI) de Asturias 2006-2009). T.F.K. acknowledges NSERC for a CGS doctoral scholarship. D.J.D. acknowledges ongoing support for this work from NSERC.

References and Notes

(1) Boom, A.; Marsalek, J. *Sci. Total Environ.* **1988**, *74*, 133.
(2) Franz, T. P.; Eisenreich, S. J. *J. Great Lakes Res.* **2000**, *26*, 220.
(3) Hautala, E. L.; Rekila, R.; Tarhanen, J.; Ruuskanen, J. *Environ. Pollut.* **1995**, *87*, 45.
(4) Herbert, B. M. J.; Villa, S.; Halsall, C. *Ecotoxicol. Environ. Saf.* **2006**, *63*, 3.
(5) Reinosdotter, K.; Viklander, M.; Malmqvist, P. A. *Water Sci. Technol.* **2006**, *54*, 195.
(6) Schondorf, T.; Herrmann, R. *Nordic Hydrology* **1987**, *18*, 259.
(7) Schrimpff, E.; Thomas, W.; Herrmann, R. *Water, Air, Soil Pollut.* **1979**, *11*, 481.
(8) Sharma, M.; McBean, E. A. *Environ. Sci. Pollut. Res.* **2001**, *8*, 11.
(9) Viskari, E. L.; Rekila, R.; Roy, S.; Lehto, O.; Ruuskanen, J.; Karenlampi, L. *Environ. Pollut.* **1997**, *97*, 153.
(10) Carrera, G.; Fernandez, P.; Vilanova, R. M.; Grimalt, J. O. *Atmos. Environ.* **2001**, *35*, 245.
(11) Cincinelli, A.; Stortini, A. M.; Checchini, L.; Martellini, T.; Del Bubba, M.; Lepri, L. *J. Environ. Monit.* **2005**, *7*, 1305.
(12) Daly, G. L.; Wania, F. *Environ. Sci. Technol.* **2005**, *39*, 385.
(13) Fernandez, P.; Carrera, G.; Grimalt, J. O.; Ventura, M.; Camarero, L.; Catalan, J.; Nickus, U.; Thies, H.; Psenner, R. *Environ. Sci. Technol.* **2003**, *37*, 3261.

(14) Fernandez, R. G.; Abascal, J. L. F.; Vega, C. *J. Chem. Phys.* **2006**, 124.
(15) Jaffrezo, J. L.; Clain, M. P.; Masclet, P. *Atmos. Environ.* **1994**, *28*, 1139.
(16) Masclet, P.; Hoyau, V.; Jaffrezo, J. L.; Cachier, H. *Atmos. Environ.* **2000**, *34*, 3195.
(17) Melnikov, S.; Carroll, J.; Gorshkov, A.; Vlasov, S.; Dahle, S. *Sci. Total Environ.* **2003**, *306*, 27.
(18) Slater, J. F.; Currie, L. A.; Dibb, J. E.; Benner, B. A. *Atmos. Environ.* **2002**, *36*, 4463.
(19) Wang, X. P.; Xu, B. Q.; Kang, S. C.; Cong, Z. Y.; Yao, T. D. *Atmos. Environ.* **2008**, *42*, 6699.
(20) Wang, X. P.; Yao, T. D.; Wang, P. L.; Yang, W.; Tian, L. D. *Sci. Total Environ.* **2008**, *394*, 134.
(21) Welch, H. E.; Muir, D. C. G.; Billeck, B. N.; Lockhart, W. L.; Brunskill, G. J.; Kling, H. J.; Olson, M. P.; Lemoine, R. M. *Environ. Sci. Technol.* **1991**, *25*, 280.
(22) Dubowski, Y.; Hoffmann, M. R. *Geophys. Res. Lett.* **2000**, *27*, 3321.
(23) Grannas, A. M.; Bausch, A. R.; Mahanna, K. M. *J. Phys. Chem. A* **2007**, *111*, 11043.
(24) Grannas, A. M.; Jones, A. E.; Dibb, J.; Ammann, M.; Anastasio, C.; Beine, H. J.; Bergin, M.; Bottenheim, J.; Boxe, C. S.; Carver, G.; Chen, G.; Crawford, J. H.; Domine, F.; Frey, M. M.; Guzman, M. I.; Heard, D. E.; Helmig, D.; Hoffmann, M. R.; Honrath, R. E.; Huey, L. G.; Hutterli, M.; Jacobi, H. W.; Klan, P.; Lefer, B.; McConnell, J.; Plane, J.; Sander, R.; Savarino, J.; Shepson, P. B.; Simpson, W. R.; Sodeau, J. R.; von Glasow, R.; Weller, R.; Wolff, E. W.; Zhu, T. *Atmos. Chem. Phys.* **2007**, *7*, 4329.
(25) Kahan, T. F.; Donaldson, D. J. *J. Phys. Chem. A* **2007**, *111*, 1277.
(26) Kahan, T. F.; Donaldson, D. J. *Environ. Res. Lett.* **2008**, *3*, 045006.
(27) Klan, P.; Holoubek, I. *Chemosphere* **2002**, *46*, 1201.
(28) Klan, P.; Klanova, J.; Holoubek, I.; Cupr, P. *Geophys. Res. Lett.* **2003**, *30*, 46.
(29) Klanova, J.; Klan, P.; Heger, D.; Holoubek, I. *Photochem. Photobiol. Sci.* **2003**, *2*, 1023.
(30) Klanova, J.; Klan, P.; Nosek, J.; Holoubek, I. *Environ. Sci. Technol.* **2003**, *37*, 1568.
(31) Matykiewiczova, N.; Kurkova, R.; Klanova, J.; Klan, P. *J. Photochem. Photobiol., A* **2007**, *187*, 24.
(32) Ram, K.; Anastasio, C. *Atmos. Environ.* **2009**, *43*, 2252.
(33) Kahan, T. F.; Reid, J. P.; Donaldson, D. J. *J. Phys. Chem. A* **2007**, *111*, 11006.
(34) Kawakubo, T.; Okada, M.; Shibata, T. *J. Phys. Soc. Jpn.* **1966**, *21*, 1469.
(35) Chandross, E. A.; Dempster, C. J. *J. Am. Chem. Soc.* **1970**, *92*, 704.
(36) Horiguchi, R.; Iwasaki, N.; Maruyama, Y. *J. Phys. Chem.* **1987**, *91*, 5135.
(37) Wei, X.; Miranda, P. B.; Shen, Y. R. *Phys. Rev. Lett.* **2001**, *86*, 1554.
(38) Benjamin, I. *Chem. Rev.* **2006**, *106*, 1212.
(39) Gopalakrishnan, S.; Liu, D.; Allen, H. C.; Kuo, M.; Shultz, M. J. *Chem. Rev.* **2006**, *106*, 1155.
(40) Winter, B.; Faubel, M. *Chem. Rev.* **2006**, *106*, 1176.
(41) Shen, Y. R.; Ostroverkhov, V. *Chem. Rev.* **2006**, *106*, 1140.
(42) Groenzin, H.; Li, I.; Buch, V.; Shultz, M. J. *J. Chem. Phys.* **2007**, *127*, 214502.
(43) Groenzin, H.; Li, I.; Shultz, M. J. *J. Chem. Phys.* **2008**, 128.
(44) Bolton, K.; Pettersson, J. B. C. *J. Phys. Chem. B* **2000**, *104*, 1590.
(45) Ikeda-Fukazawa, T.; Kawamura, K. *J. Chem. Phys.* **2004**, *120*, 1395.
(46) Kroes, G.-J. *Surf. Sci.* **1992**, *275*, 365.
(47) Mantz, Y. A.; Geiger, F. M.; Molina, L. T.; Molina, M. J.; Trout, B. L. *J. Chem. Phys.* **2000**, *113*, 10733.
(48) Materer, N.; Starke, U.; Barbieri, A.; VanHove, M. A.; Somorjai, G. A.; Kroes, G. J.; Minot, C. *Surf. Sci.* **1997**, *381*, 190.
(49) Paesani, F.; Voth, G. A. *J. Phys. Chem. C* **2008**, *112*, 324.
(50) Picaud, S.; Hoang, P. N. M. *J. Chem. Phys.* **2000**, *112*, 9898.
(51) Collignon, B.; Picaud, S. *Chem. Phys. Lett.* **2004**, *393*, 457.
(52) Picaud, S.; Hoang, P. N. M.; Peybernes, N.; Le Calve, S.; Mirabel, P. *J. Chem. Phys.* **2005**, 122.
(53) Domine, F.; Cincinelli, A.; Bonnaud, E.; Martellini, T.; Picaud, S. *Environ. Sci. Technol.* **2007**, *41*, 6033.
(54) Conde, M. M.; Vega, C.; Patrykiejew, A. *J. Chem. Phys.* **2008**, 129.
(55) Berendsen, H. J. C.; Postma, J. P. M.; Vangunsteren, W. F.; Dinola, A.; Haak, J. R. *J. Chem. Phys.* **1984**, *81*, 3684.
(56) Ryckaert, J. P.; Ciccotti, G.; Berendsen, H. J. C. *J. Comput. Phys.* **1977**, *23*, 327.
(57) Essmann, U.; Perera, L.; Berkowitz, M. L.; Darden, T.; Lee, H.; Pedersen, L. G. *J. Chem. Phys.* **1995**, *103*, 8577.
(58) Vacha, R.; Jungwirth, P.; Chenb, J.; Valsaraj, K. *Phys. Chem. Chem. Phys.* **2006**, *8*, 4461.
(59) Vacha, R.; Cwiklik, L.; Rezac, J.; Hobza, P.; Jungwirth, P.; Valsaraj, K.; Bahr, S.; Kempter, V. *J. Phys. Chem. A* **2008**, *112*, 4942.
(60) Duan, Y.; Wu, C.; Chowdhury, S.; Lee, M. C.; Xiong, G. M.; Zhang, W.; Yang, R.; Cieplak, P.; Luo, R.; Lee, T.; Caldwell, J.; Wang, J. M.; Kollman, P. *J. Comput. Chem.* **2003**, *24*, 1999.
(61) Bayly, C. I.; Cieplak, P.; Cornell, W. D.; Kollman, P. A. *J. Phys. Chem.* **1993**, *97*, 10269.
(62) Case, D. A.; Darden, T. A.; Cheatham, T. E.; Simmerling, C. L.; Wang, J.; Duke, R. E.; Luo, R.; Crowley, M.; Walker, R. C.; Zhang, W.; Merz, K. M.; Wang, B.; Hayik, S.; Roitberg, A.; Seabra, G.; Kolssrary, I.; Wong, K. F.; Paesani, F.; Vanicek, J.; Wu, X.; Brozell, S. R.; Steinbrecher, T.; Gohlke, H.; Yang, L.; Tan, C.; Mongan, J.; Hornak, V.; Cui, G.; Mathews, D. H.; Seetin, M. G.; Sagui, C.; Babin, V.; Kollman, P. A. *AMBER*, 10 ed; University of California: San Francisco, CA, 2008.
(63) Sato, T.; Tsuneda, T.; Hirao, K. *J. Chem. Phys.* **2005**, 123.
(64) Kumar, S.; Bouzida, D.; Swendsen, R. H.; Kollman, P. A.; Rosenberg, J. M. *J. Comput. Chem.* **1992**, *13*, 1011.
(65) Kumar, S.; Rosenberg, J. M.; Bouzida, D.; Swendsen, R. H.; Kollman, P. A. *J. Comput. Chem.* **1995**, *16*, 1339.
(66) Saeki, M.; Akagi, H.; Fujii, M. *J. Chem. Theory Comput.* **2006**, *2*, 1176.
(67) Petersen, P. B.; Saykally, R. J. *Annu. Rev. Phys. Chem.* **2006**, *57*, 333.

JP811385M